

Supplemental material

Michaux et al., <https://doi.org/10.1083/jcb.201806161>

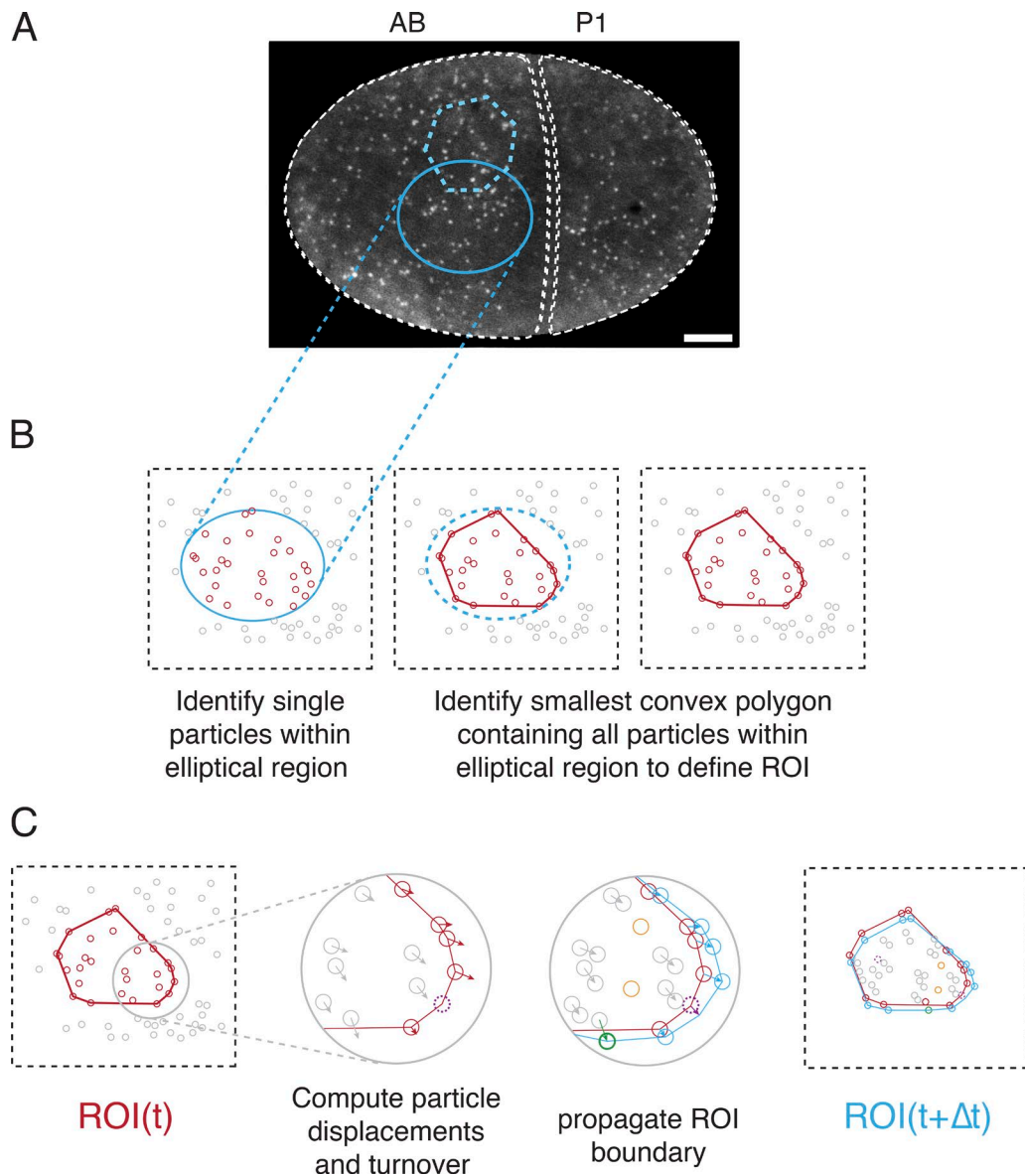


Figure S1. **Schematic overview of methods for tracking a moving and deforming patch of cortex from single-molecule data (related to Fig. 2).** **(A)** Micrograph of a two-cell stage embryo expressing Actin::GFP at single-molecule levels. Anterior is to the left. Dashed lines indicate the outlines of AB and P1. The blue ellipse identifies a region in which a pulse occurs, from which a "reference ROI" will be extracted. Bar, 5 μm . **(B)** Method for extracting the reference ROI. Left: Single particles detected in the raw image. The particles shown in red are those contained within the blue ellipse. Middle and right: The reference ROI (solid red line) is the smallest convex polygon containing all red particles. **(C)** Strategy for iterative propagation of the polygonal ROI from frame to frame (either backward or forward in time). The polygon's vertices move with the particle that defined that vertex so long as the particle remains visible. When a particle associated with a vertex disappears (dashed magenta particle in middle left panel), the vertex displacement is extrapolated from the motion of the surrounding particles. If an internal particle moves outside the boundaries of the polygon defined by existing vertices (green particle in middle right panel), a new vertex associated with that particle is introduced.

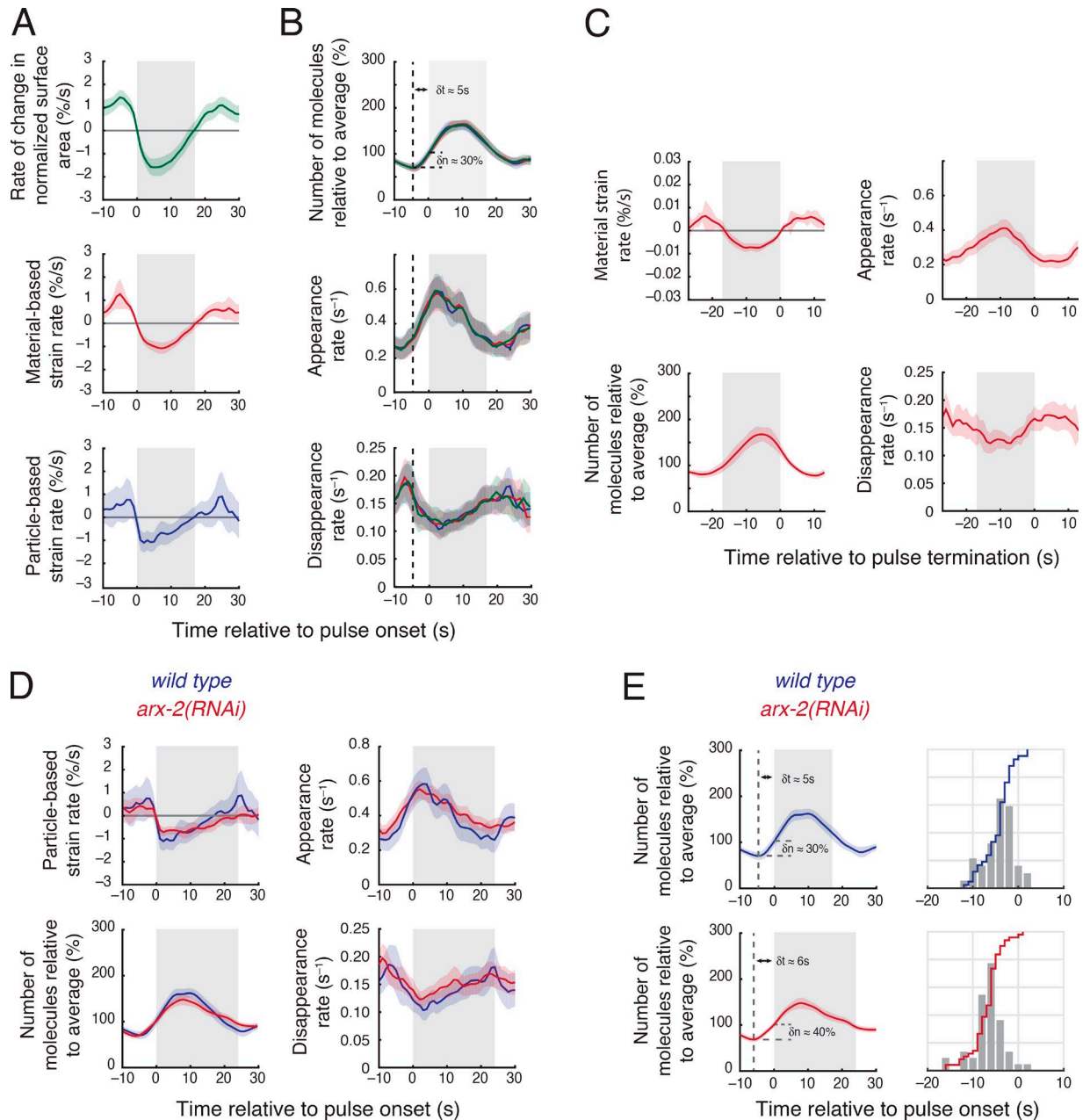


Figure S2. **Comparison of different methods to quantify local deformation (strain rate) and to align data across multiple pulses (related to Fig. 3).** **(A and B)** Comparison of different methods used to compute local deformation rates during pulses. **(A)** Measures of deformation rate versus time for the same data by using three different metrics: top, rate of change in normalized surface area; middle, material strain rate; and bottom, particle based strain rate (see Materials and methods for details on how these were computed). **(B)** Measurements of the single-molecule number (top), appearance rate (middle), and disappearance rate (bottom) were aligned and averaged with respect to the onset of contraction, over 42 pulses, by using the three metrics to measure deformation: change in normalized surface area (green), material strain rate (red), and particle-based strain rate (blue). Vertical dashed lines mark lowest actin density preceding the pulse. Horizontal dashed lines in the top graph mark, respectively, the minimum number of actin molecules and the number of molecules at the onset of contraction. For all three metrics, the delay from actin minimum to contraction onset is $\delta t \approx 30\%$. **(C)** Measurements of material strain rate, number of molecules, appearance rate and disappearance rate, aligned and averaged with respect to the end of contraction for the same data shown in A and B. **(D)** Measurements of particle-based strain rate, number of molecules, appearance rate and disappearance rate, aligned and averaged with respect to the onset of contraction, in wild-type (blue, $n = 42$ pulses) and *arx-2(RNAi)* (red, $n = 49$ pulses) embryos. **(E)** Left column: Number of molecules relative to average in wild-type (blue) and *arx-2(RNAi)* (red) embryos, as displayed in D. The vertical dashed line marks the lowest actin density preceding the pulse delayed, respectively, by $\delta t \approx 5$ s and $\delta t \approx 6$ s from the contraction onset (gray box). The horizontal dashed line displays the amount of precontraction increase in the number of actin molecules, with $\delta n \approx 30\%$ and $\delta n \approx 40\%$. Right column: a histogram showing the distribution of delays between contraction onset and increase of actin molecules. Staircase line: cumulative distribution function of the delays. Error bars indicate 95% confidence intervals.

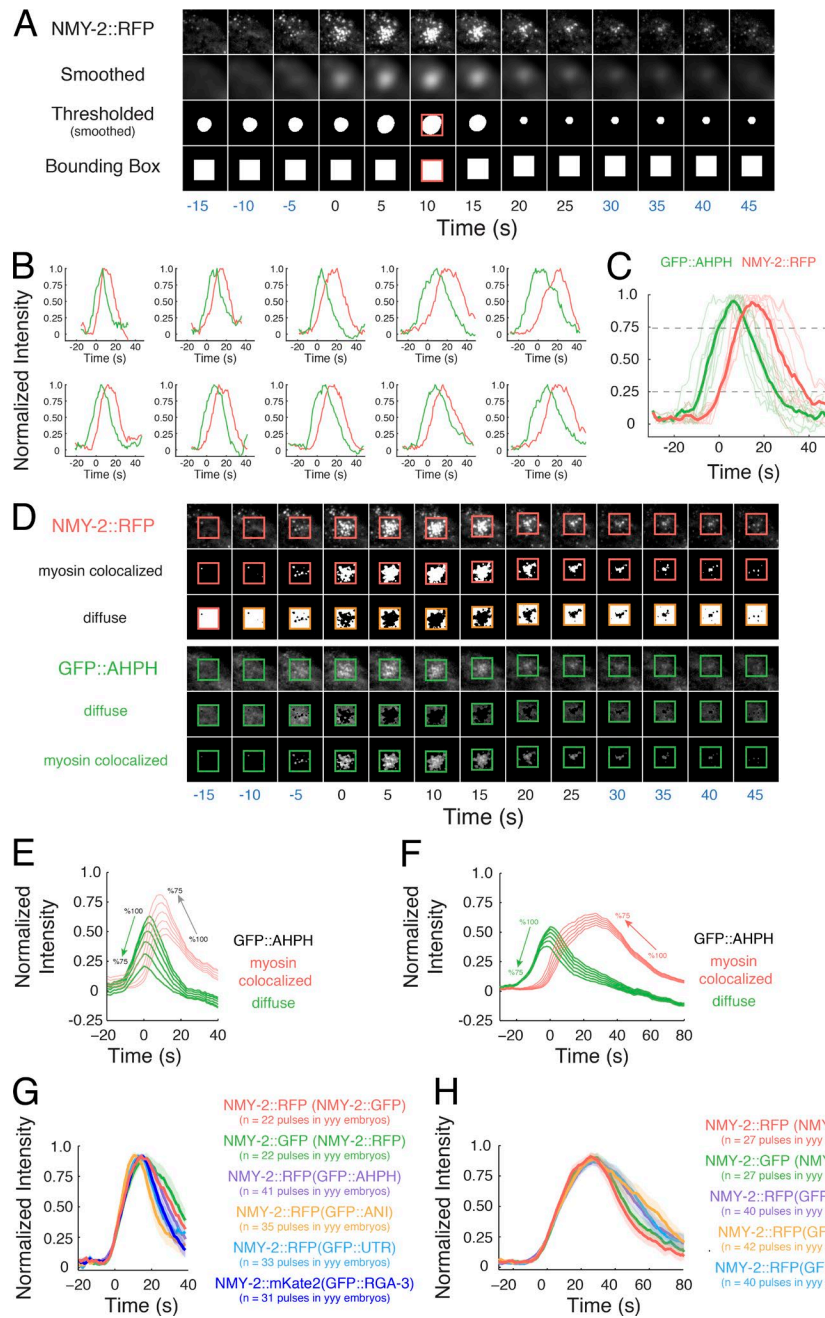


Figure S3. **Measurement, alignment, and decomposition of fluorescence intensity data during pulsed contractions (related to Fig. 4).** **(A)** Method for determining regions of interest in which to measure fluorescence intensities, illustrated for a single pulse. Row 1: Raw NMY-2::RFP signal. Row 2: Smoothed NMY-2::RFP signal. Row 3: Smoothed and thresholded NMY-2::RFP signal. Row 4: The bounding box is defined to be the smallest rectangular region containing the largest thresholded domain (red box at time = 10). In each frame, the center of bounding box is located on the centroid of the thresholded domain. **(B)** Normalized fluorescence intensity of GFP::AHPH and NMY-2::RFP versus time for ten representative pulses in AB cells. Time $t = 0$ is when NMY-2::RFP rises above 25% of its normalized maximum value. **(C)** Fluorescence intensities from all pulses in B coaligned relative to time $t = 0$. The bold traces represent the average GFP::AHPH and NMY-2::RFP intensities. **(D)** Method for decomposing the GFP::AHPH signal into diffuse and myosin-colocalized pools, illustrated for a single pulse. In rows 1–6, the colored box represents the outline of the bounding box region determined in panel A, row 4. Row 1: Raw NMY-2::RFP signal. Row 2: Myosin-colocalized mask obtained by thresholding the raw NMY-2::RFP signal. Here, NMY-2::RFP was thresholded at 95% of its maximum intensity. Row 3: Diffuse mask obtained by subtracting the myosin-colocalized mask from the bounding box region determined in row 5 of Fig. S3. Row 4: Raw GFP::AHPH signal. Row 5: Diffuse GFP::AHPH signal. Row 6: Myosin-colocalized GFP::AHPH signal. **(E and F)** Averaged normalized fluorescence intensity of GFP::AHPH measured in the diffuse (green) and myosin-colocalized (gray) regions for pulses in AB (E) and P0 (F) cells. The arrows indicate how the intensity curves for the diffuse and myosin-colocalized pools change as the NMY-2::RFP threshold level is changed. Data in E were averaged over 41 pulses in seven embryos. Data in F were averaged over 40 pulses in four embryos. **(G and H)** Alignment of averaged normalized fluorescence intensities for NMY-2::XFP measured for pulses in P0 (G) and AB (H) cells coexpressing the indicated probes. Time $t = 0$ is when NMY-2::XFP rises above 25% of its normalized maximum value. Text below graphs in G and H indicates the number of embryos and pulses used to compute averages for each genotype. In C, G, and H, halos report 95% confidence intervals.

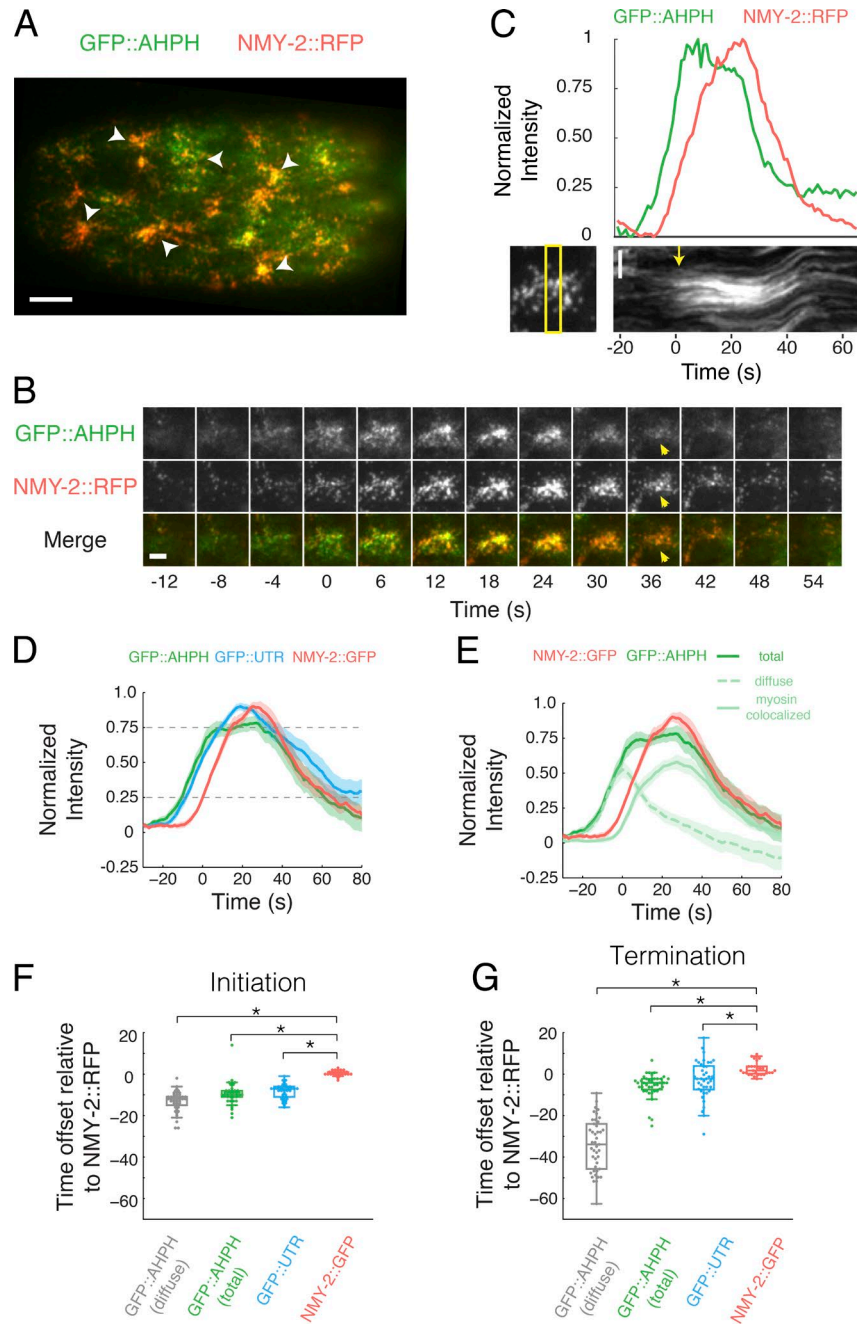


Figure S4. **Two-color analysis of pulsed contractions in P0 (related to Fig. 4).** (A) A zygote expressing GFP::AHPH and NMY-2::RFP. White arrowheads indicate individual pulses. (B) Expanded view of a single pulse illustrating temporal dynamics of GFP::AHPH and NMY-2::RFP accumulation. Time delay between frames is 4 s for the first four frames and 6 s thereafter. (C) Plot of normalized fluorescence intensities of GFP::AHPH and NMY-2::RFP versus time for the pulse displayed in B. Bottom: Kymograph showing movements of NMY-2::RFP puncta before and during the pulse. Yellow box at left indicates the region used to make the kymograph. The yellow arrow at the right indicates the onset of contraction. Note that a sharp rise in GFP::AHPH precedes both myosin accumulation and onset of contraction. (D) Averaged normalized fluorescence intensities for NMY-2::RFP, GFP::AHPH, and GFP::UTR from two-color videos, aligned to the time at which NMY-2::RFP reaches the 25% threshold. Shaded areas represent 95% confidence intervals. (E) Decomposition of the GFP::AHPH signal into diffuse (gray, dashed line) and myosin-colocalized (gray, solid line) pools. Shaded areas represent 95% confidence intervals. (F) Distributions of the delay in the onset of accumulation of GFP::AHPH, GFP::UTR, and NMY-2::GFP, measured relative to the onset of accumulation of NMY-2::RFP during pulse initiation for many individual pulses. The onset of accumulation is measured as the time at which each normalized signal exceeds 25% of its maximum value. (G) Distributions of the delay in the onset of disappearance of GFP::AHPH, GFP::UTR, and NMY-2::GFP measured relative to NMY-2::RFP during pulse termination for many individual pulses. The onset of disappearance is measured as the time at which each normalized signal falls below 75% of its maximum value. Data in D–G were averaged over the following—GFP::AHPH: $n = 40$ pulses in four embryos; GFP::UTR: $n = 40$ pulses in three embryos; NMY-2::GFP: $n = 27$ pulses in three embryos. For the box plots in F and G, the central mark represents the median, the box indicates the 25th and 75th percentile, the whiskers mark the minimum and maximum values, the + represents outliers, and * indicates statistically significant differences with $P < 0.01$. Bars: (A) 5 μm ; (B and C) 2 μm .

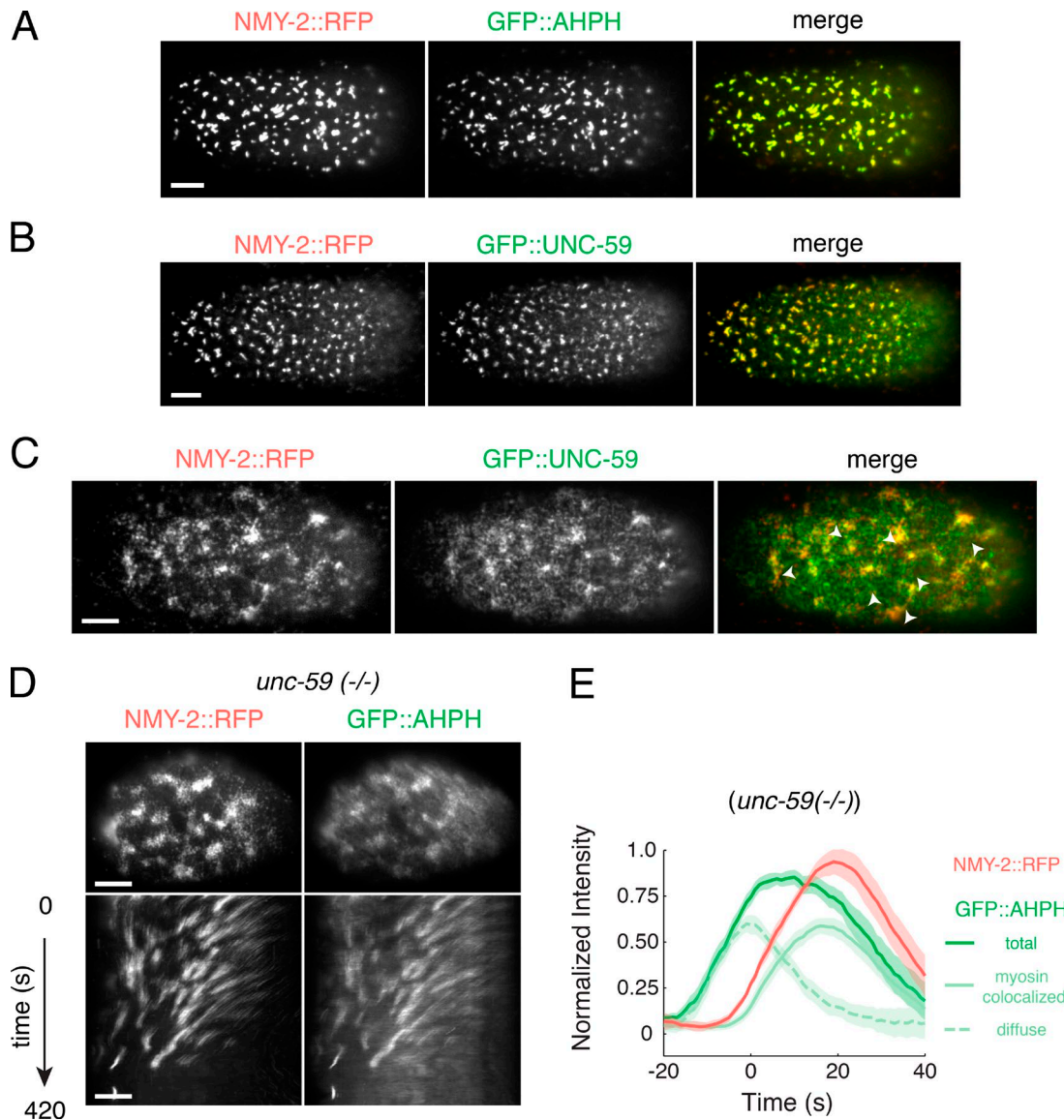
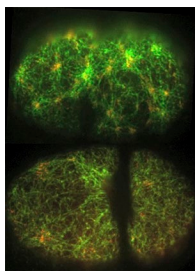
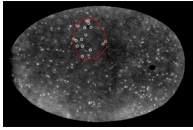


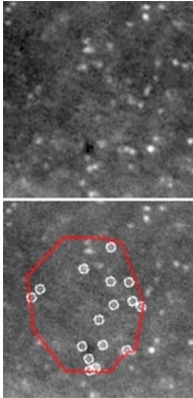
Figure S5. **Septin localization and contributions to pulsed contractions in one-cell embryos (related to Fig. 9).** (A and B) Zygotes coexpressing NMY-2::RFP and either GFP::AHPH (A) or GFP::UNC-59 (B) after acute treatment with 10 μ M LatA. Merged images show coclustering of Myosin II, GFP::AHPH, and GFP::UNC-59. Data in A and B are representative of more than six individual experiments. (C) A zygote coexpressing NMY-2::RFP (left) and GFP::UNC-59 (middle). White arrowheads in the merged (right) image indicate individual pulses. (D) Single frames (top) and kymographs (bottom) showing NMY-2::RFP and GFP::AHPH dynamics in *unc-59(e261)* zygotes. (E) Plots of averaged normalized fluorescence intensities for GFP::AHPH and NMY-2::RFP in *unc-59(e261)* embryos from two-color videos, aligned to the time at which NMY-2::RFP reaches the 25% threshold. Data in E were averaged over 40 pulses in four embryos. Shaded areas represent 95% confidence intervals. Bars, 5 μ m.



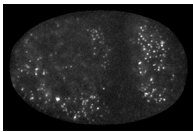
Video 1. **Actomyosin pulse dynamics in wild-type cells expressing GFP::UTR and NMY-2::RFP (related to Fig. 1).** Top: A wild-type P0 during interphase as polarity is established. Bottom: The two-cell embryo shortly after cell division when both the AB and the posterior blastomere P1 are in interphase. Anterior is to the left in this and all subsequent videos. Time compression = 15:1.



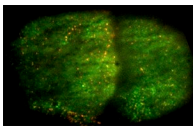
Video 2. **Two-cell embryo expressing GFP::ACT-1 at single-molecule levels and imaged in near-TIRF mode (related to Fig. 2).** Each frame is the average of 10 consecutive images collected with 100-ms exposures. Time compression = 15:1.



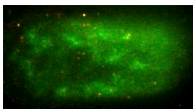
Video 3. **Dynamic tracking of a cortical patch from single-molecule data (related to Fig. 2).** The video focuses on a rectangular subregion of the AB cortex $14.5 \times 15 \mu\text{m}$ from the same embryo shown in Video 2. Top: The raw data; bottom: white circles highlight tracked particles, and the dashed polygon outlines the tracked boundary of the cortical patch. See Materials and methods for details. Time compression = 15:1.



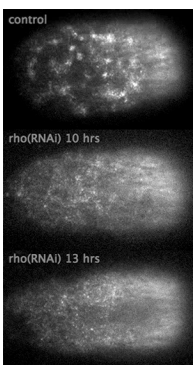
Video 4. **Two-cell embryo expressing NMY-2::GFP at single-molecule levels and imaged in near-TIRF mode (related to Fig. 3).** Each frame is the average of 10 consecutive images collected with 100-ms exposures. Time compression = 15:1.



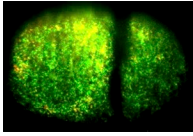
Video 5. **Pulse dynamics in a two-cell embryo expressing GFP::AHPH and NMY-2::RFP (related to Fig. 4).** GFP::AHPH is in the green channel; NMY-2::RFP is in the red channel. Each frame is the average of five consecutive frames collected with 200-ms exposures. Time compression = 15:1.



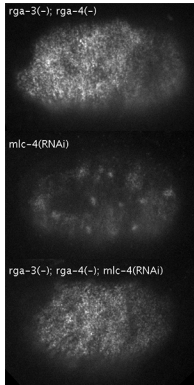
Video 6. **Pulse dynamics in a zygote expressing GFP::AHPH and NMY-2::mKate and subjected to strong *nmy-2* RNAi (related to Fig. 5).** GFP::AHPH is in the green channel; NMY-2::mKate is in the red channel. Time compression = 15:1.



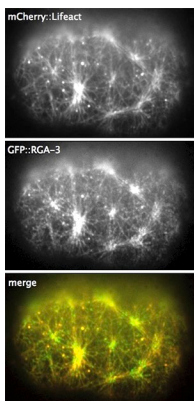
Video 7. **Pulse dynamics in zygotes expressing GFP::AHPH and subjected to *rho-1* RNAi for different periods of time (related to Fig. 7).** Top: Control; middle: 10 h of feeding; bottom: 13 h of feeding. Time compression = 30:1.



Video 8. **Dynamics of GFP::RGA-3 and NMY-2::RFP accumulation during pulsing in AB cells (related to Fig. 8).** GFP::RGA-3 is in the green channel; NMY-2::RFP is in the red channel. Time compression = 15:1.



Video 9. **Absence of RhoA pulsing in *rga-3*; *rga-4* double mutants (related to Fig. 8).** Top: *rga-3*; *rga-4* double-mutant zygote. Middle: Control (*rga-3*/+; *rga-4*/+) zygote partially depleted of MLC-4 by RNAi (12–16 h of feeding). Bottom: *rga-3*; *rga-4* double-mutant zygote partially depleted of MLC-4 by RNAi (12–16 h of feeding). Time compression = 30:1.



Video 10. **Coordinated response of cortical F-actin and RGA-3 to acute treatment with LatA (related to Fig. 9).** Zygote co-expressing GFP::RGA-3 and mCherry::Lifeact. Top: mCherry::Lifeact; middle: GFP::RGA-3; bottom: two-color merge. The bright flash indicates the time at which LatA was applied. Time compression = 15:1.